

ADHESION AND UNBINDING OF VESICLES

Udo Seifert[†] and *Reinhard Lipowsky*[‡]

[†] Department of Physics, Simon Fraser University, Burnaby, B.C., V5A 1S6, Canada

[‡] Institut für Festkörperforschung, Forschungszentrum Jülich, 5170 Jülich, Germany

Abstract. We discuss theoretical predictions for the adhesion of vesicles to a wall which can be a substrate, another membrane or an interface. In a simple model with a contact potential, the interplay between bending and adhesion energy leads to a variety of bound states and to a curvature driven adhesion transition which can be continuous or discontinuous. In a potential with finite range, this transition separates the bound state with finite contact area from a state in which the vesicle assumes its free shape but is pinned by the potential minimum. Thermally excited fluctuations are shown to promote two different unbinding transitions: Small vesicles unbind by thermal activation while larger vesicles unbind via shape fluctuations. We also discuss the validity of the Young-Dupré equation, lateral tension as well as topological changes induced by adhesion such as fusion and rupture.

1. Introduction

Adhesion plays a central role in many biological and biophysical processes: Mutual adhesion of cells leads to the formation of tissue. Various transport processes involve the adhesion of vesicles to cell surfaces. Drug delivery by liposomes is an example for a biotechnological application. These systems typically involve objects with many components and represent states far from equilibrium.

Adhesion, however, also occurs for simple configurations such as mutual adhesion of artificial vesicles which can be studied with micropipet aspiration techniques [1]. Accidental adhesion in dilute systems can be investigated by light microscopy [2].

In general, adhesion of closed vesicles leads to a change in their shape which costs bending energy, and will, thus, only occur if this loss (and the loss in translational

entropy) is compensated by a gain in adhesion energy. We discuss the consequences of a theoretical model [3-6] which focuses on this aspect.

2. The model

Since a typical membrane has a thickness in the nm -range and lateral extension in the μm -range, it can be regarded as a two-dimensional surface embedded in three-dimensional space. Fluid membranes have no internal connectivity and therefore no elastic energy associated with displacements within the surface. The relevant energy arises solely from the bending of the membrane which is governed by the curvature of the embedded shape [7-9].

A vesicle near a wall experiences various kind of forces, such as van der Waals and hydration forces. The typical range of these forces is in the nm -range and may, in a first step, be replaced by a contact potential with strength W . The curvature and the adhesion term then lead to the energy [3]

$$F \equiv (\kappa/2) \oint (2H)^2 dA + \kappa_G \oint C_1 C_2 dA - WA^*. \quad (1)$$

Here, $H \equiv (C_1 + C_2)/2$ is the mean curvature and $C_1 C_2$ is the Gaussian curvature in terms of the inverse radii of curvature C_1 and C_2 . The two bending rigidities κ and κ_G have the dimension of energy. The last term accounts for the adhesion energy which is proportional to the contact area A^* .

As for free vesicles, the energy F has to be minimized subject to constraints for the total area A , the enclosed volume V and the total mean curvature $M \equiv \oint dA H$. The latter constraint is physically equivalent to fixing the area difference between the two monolayers [10]. Such a constraint applies to real bilayers provided one can ignore the exchange of lipid molecules (flip-flop) between the two monolayers. If the constraints are added to (1) by Lagrangian multipliers, the minimization leads to shape equations and boundary conditions. The adhesion term $-WA^*$ enters only the boundary conditions:

(i) The contact angle is π since any sharp bent would imply an infinite curvature energy. (ii) The contact curvature C_1^* is determined by [3]

$$C_1^* = (2W/\kappa)^{1/2}, \quad (2)$$

while $C_2^* = 0$. This universal condition holds irrespective of the size of the vesicle or the constraints imposed. Thus, a measurement of C_1^* would lead to a value for the contact potential once the bending rigidity κ is known.

3. Adhesion transition and phase diagrams

Solving the shape equations for axisymmetric shapes with the boundary condition (2) leads to a variety of bound shapes. It is convenient to discuss the results for different number of constraints imposed subsequently.

First, consider the case where only the area $A \equiv 4\pi R^2$ is fixed [3]. Physically, this corresponds to experiments on long time scales where the volume may equilibrate by the exchange of water. With decreasing W , the area of contact A^* also decreases and vanishes for $W = W_a$, with

$$W_a = 2\kappa/R^2. \quad (3)$$

At this value, the bound shape assumes the free shape corresponding to the same constraint which is a sphere. For $W < W_a$, an attractive potential does not lead to a bound shape with finite area of contact. Thus, a continuous adhesion transition occurs at $W = W_a$.

This transition implies that, for fixed W , in an ensemble of vesicles only those vesicles with $R > R_a = (2\kappa/W)^{1/2}$ are bound.

Second, consider the area-volume ensemble in which both area A and the volume V are prescribed. For free vesicles, the phase diagram depends only on the reduced volume

$$v \equiv V/(4\pi R^3/3). \quad (4)$$

In this case, three different regimes are separated by discontinuous transitions [11]: The shapes of minimal energy are: (i) the cup-shaped stomatocytes for $0 < v \lesssim 0.59$, (ii) the biconcave discocytes (which evolve from the convex oblates) for $0.59 \lesssim v \lesssim 0.65$ and (iii) the dumbbells and prolates for $0.65 \lesssim v < 1$.

In the presence of a wall, the phase diagram [4,5] and several bound shapes are shown in Fig.1. The phase diagram becomes two-dimensional and depends on v and the reduced potential strength $w \equiv WR^2/\kappa$.

The stomatocytes undergo a continuous transition C_a^{sto} at $W = W_a = w_a(v)\kappa/R^2$. For the discocytes, the adhesion transition is discontinuous, i.e., we find coexistence of a bound shape with finite area of contact and a free shape along D_a^{ob} . As a consequence, for $v \gtrsim 0.52$, the continuous adhesion transition for the stomatocytes is preempted by a discontinuous transition D_a^{sto} . Moreover, there is a discontinuous transition D between bound discocytes and bound stomatocytes.

The dumbbells and prolates undergo a discontinuous transition D_a^{pro} to bound oblates if one ignores non-axisymmetric bound shapes. An investigation of this possibility would require the solution of the non-axisymmetric shape equation (a fourth order non-linear partial differential equation) with moving boundaries. However, some insight into the relevance of non-axisymmetric bound shapes can be obtained as follows.

The critical value W_a for the *continuous* adhesion transition for the stomatocytes and the oblates (not appearing in the phase diagram) obeys the condition that for $A^* \rightarrow 0$, the contact mean curvature of the bound shape, $H^* \equiv (C_1^* + C_2^*)/2 = C_1^*/2$, becomes identical to the mean curvature H_f of the corresponding free shape at this point of contact. Using (2) this condition locates the *continuous* adhesion transition at

$$W_a = 2\kappa H_f^2. \quad (5)$$

For a sphere, one has $H_f = 1/R$ which leads to (3).

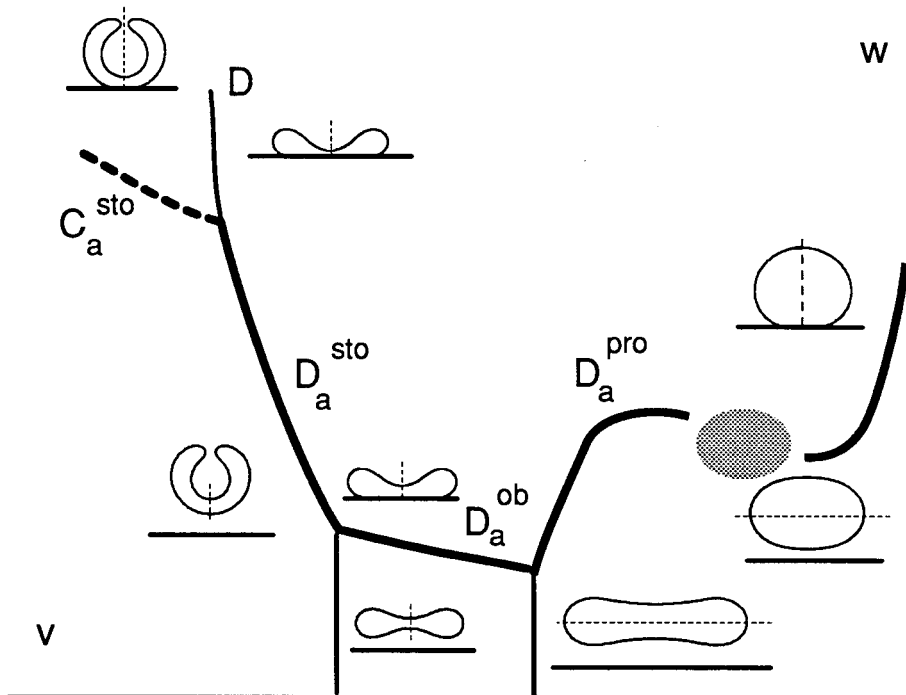


Fig.1: Schematic phase diagram with free and bound shapes in the A, V -ensemble. The heavy lines show the adhesion transition at $W = W_a$, which can be discontinuous (D_a^{pro}, D_a^{ob} and D_a^{sto}) or continuous (C_a^{sto}). In the dashed region, non-axisymmetric bound shapes are relevant. The dashed straight lines across the shapes denote axes of symmetry.

If we assume that the condition (5) is also valid for a (hypothetical) continuous transition of the prolates and dumbbells (with their axis of symmetry parallel to the wall), we can compare the energy at this transition with the energy of a bound oblate at the same v and w investigated so far. Such a comparison shows that in a small region around $v \simeq 0.90$ the non-axisymmetric bound shapes have indeed lower energy. It remains to be seen whether the adhesion transition to these states is continuous at $W_a = 2\kappa H_f^2$ (where H_f is the mean curvature at the equator of the prolate) or discontinuous at $W_a < 2\kappa H_f^2$ and how far this region of non-axisymmetric bound shapes extends. With increasing W , these non-axisymmetric states should then undergo a transitions to axisymmetric bound shapes.

Finally, consider the case where all three constraints on A, V and M are imposed which defines the bilayer coupling model for adhesion. The phase diagram for the free vesicles is now two-dimensional and includes pear-shaped vesicles and non-axisymmetric shapes (which are ellipsoidal with three different axis for $v \lesssim 1$) [11,12]. The three-dimensional adhesion diagram has not yet been fully explored. In analogy

to the free case, one expects that the additional constraint on M favours continuous adhesion transitions which would occur at $W_a = 2\kappa H_f^2$ with the corresponding H_f .

4. Strong adhesion: Young-Dupré limit and tension

The adhesion transition takes place for $R = R_a = (w_a \kappa / W)^{1/2}$, where w_a is a numerical coefficient of $O(1)$ which depends on the constraints. For large vesicles with $R \gg R_a$, i.e. for strong adhesion, the shape of the bound vesicle approaches a simple limit shape. If only the area is constrained, this limit shape is a pancake with an energy [5]

$$F \approx -2\pi W R^2 + 2\pi g(2\kappa W)^{1/2} R, \quad (6)$$

where $g \simeq 2.8$. If in addition the volume is constrained, the vesicle becomes a spherical cap for strong adhesion. In both cases, an *effective contact angle* Ψ_{eff} can be defined which obeys a Young-Dupré equation [3]

$$W = \Sigma(1 + \cos \Psi_{eff}). \quad (7)$$

For the pancake, one has $\Psi_{eff} = 0$.

The quantity Σ in (7) is the (numerical) value of the Lagrange multiplier for the area constraint. It also obeys the relation $\Sigma = \partial F / \partial A$ at constant V . Although it is tempting to identify Σ with a lateral tension, this is not justified a priori since we are dealing so far with an incompressible membrane of fixed area.

Real membranes have a finite compressibility which leads to an additional elastic term

$$F_k \equiv (k/2)(A - A_0)^2 / A_0 \quad (8)$$

in the energy (1) where k is the area compressibility modulus of the order of $10^{-13} J/\mu m^2$ [13]. Such an extended model leads to the same shape equations as the model defined by (1). Even the boundary condition (2) remains unchanged. The phase diagram, however, changes due to the additional energy.

In general, adhesion induces stretching. A crude estimate of this effect can be obtained as follows: Suppose that a certain bound shape with area A_0 , contact area A_0^* and energy F_0 minimizes the energy (1) for an incompressible membrane. As a variational solution for finite compressibility, we consider the same bound shape scaled with a linear factor $(1 + \lambda)^{1/2}$. Such a shape has an energy $F(\lambda) = F_0 - W A_0^* \lambda + (k/2) A_0 \lambda^2$. Minimization with respect to λ leads to the adhesion induced stretching $\lambda_{min} = W A_0^* / (k A_0)$. The elastic lateral tension Σ_{el} follows from $\Sigma_{el} = \partial F_k / \partial A|_{\lambda=\lambda_{min}} = W A_0^* / A_0$. Since it is independent of k , it holds also in the limit of an incompressible membrane. Thus, the Lagrange multiplier Σ and the elastic tension Σ_{el} are proportional for strong adhesion and one may indeed use Σ as a (crude) measure of the tension in the membrane. For a pancake, we have $A_0^* / A_0 = 1/2$, it then follows from (7) that $\Sigma_{el} = \Sigma$ since $\Psi_{eff} = 0$ in this case.

In general, the solution of the model defined by (1) with (8) would show that the lateral tension does not coincide with the value of the Lagrange multiplier Σ used to enforce the area A_0 in the model (1) without (8).

5. Topological changes induced by adhesion: Fusion and Rupture

So far, an isolated vesicle at a wall has been considered. If more and more bound vesicles cover the wall, these come into contact and may fuse. For free vesicles, fusion of two vesicles with equal area $A \equiv 4\pi R^2$ (but no constraint on the volume) leads to a gain in energy $\Delta F_{fv} = 8\pi\kappa + 4\pi\kappa_G$. If two bound vesicles fuse, the gain in energy is always larger and satisfies $\Delta F_{bv} \geq \tilde{g}\pi\kappa + 4\pi\kappa_G$ with $\tilde{g} \simeq 8.3$. For large R , this energy gain behaves as $\Delta F_{bv} \approx 4\pi g(\sqrt{2} - 1)(\kappa W)^{1/2} R$, where (6) has been used. Thus, adhesion favours fusion [5].

The larger the fused vesicles become, the more their shape approaches the pancake. If the elastic tension exceeds the threshold for lysis, the pancake ruptures and becomes an open bound disc. Such a conformation has an energy [5]

$$F_{bd} = -4\pi W R^2 + 4\pi \Sigma_e R, \quad (9)$$

where Σ_e is the edge tension along the circumference of the bound disk. A comparison of the energy (9) with the energy (6) of a pancake shows that for $R \gg R_{bd} \equiv \Sigma_e/W$ the bound disc always has lower energy (irrespective of the value of the other parameters). For phospholipid bilayers, we find with the typical value $\Sigma_e = 5 \times 10^{-17} \text{ J}/\mu\text{m}$ the length scale $R_{bd} = 50 \mu\text{m}$ assuming moderate adhesion with $W = 10^{-18} \text{ J}/\mu\text{m}^2$.

A recent experiment has shown that a lamellar structure can form at the air-water interface of a vesicle suspension [14]. The energetic considerations discussed above immediately lead to a scenario where vesicles adhere to the wall, fuse at the wall and rupture. Finally, the open discs will also fuse, thus forming a bilayer parallel to the wall. The same experiment has also revealed that the activation barriers involved in these processes depend sensitively on temperature.

6. Adhesion in a potential with finite range

The contact potential discussed so far is an approximation to realistic interactions between the vesicle and the wall. In general, one has a potential $V(Z)$, where Z is the coordinate perpendicular to the wall. In this section, we discuss adhesion in such a potential [15] which will also be required for an investigation of the effect of fluctuations on the adhesion transition.

The adhesion energy in such a potential reads

$$F_V \equiv \oint dA V(Z) \quad (10)$$

which replaces the contact potential term $-WA^*$ in (1). For simplicity, we focus on smooth two-parameter potentials $V(Z)$ which have a repulsive core, a single minimum with depth V^0 , a typical length-scale or range Z_0 and which vanish faster than $\sim Z^{-2}$ for large Z , such as, e.g.,

$$V(Z) = V^0[(Z_0/Z)^{2n} - 2(Z_0/Z)^n], \quad (11)$$

with $n > 2$. The parametrization in (11) implies that the potential minimum is at $Z = Z_0$ and that $V(Z_0) = -V^0$.

Vesicle shapes of minimal energy in such a potential have been studied in some detail for two-dimensional vesicles [16]. Here, we extend the essential results to the three dimensional case.

Depending on the range Z_0 and on the size of the vesicle R , two limiting cases can be distinguished theoretically.

(1) For $R \lesssim Z_0$, which defines the *long-ranged* case, the whole bound vesicle is exposed to the adhesion potential F_V . The deviations from the free shape (with the same constraints) are significant, if the variation of the potential along the vesicles contour becomes comparable to the energy $F \sim \kappa$. This happens at the potential strength $V^0 = V_f^0$, which scales as

$$V_f^0 \sim \kappa Z_0^2 / R^4, \quad (12)$$

as can be estimated by expanding the potential around its minimum.

Thus, for $V_0 \ll V_f^0$, the bound vesicle has more or less its free shape and gains an energy

$$\Delta F \sim -V^0 R^2, \quad (13)$$

while for $V_0 \gtrsim V_f^0$ the adhesion potential deforms the free shape.

(2) For *short-ranged* potentials with $Z_0 \ll R$, only the adjacent part of the vesicle is exposed to the potential and one should recover the results for the contact potential case. In fact, the limiting behaviour for small Z_0/R depends on the potential strength:

(i) If V^0 is larger than the critical value, W_a , for the adhesion transition in the contact potential, the vesicle in the smooth potential $V(Z)$ approaches in the limit of small Z_0/R the same shape obtained for adhesion in a contact potential with $W = V^0$. In particular, the boundary condition (2) also evolves in this limit without being imposed.

(ii) For $V^0 < W_a$, on the other hand, the vesicle approaches in the same limit the free shape (satisfying the same constraints). It remains, however, pinned in the (narrow) potential minimum up to the limit $Z_0 = 0$ where it is pinned in one point (in the absence of thermal fluctuations). Indeed, the area which is actually exposed to the potential well vanishes as $Z_0 R$, which leads to the energy gain

$$\Delta F \sim -V^0 R^2 (Z_0/R), \quad (14)$$

for small Z_0/R in the pinned state.

Thus, if the adhesion transition found in a contact potential has been discontinuous, the finite range Z_0 leads to a transition between the bound and the pinned state at

$$V^0 = V_a^0(Z_0, R), \quad \text{with} \quad V_a^0(0, R) = W_a. \quad (15)$$

With increasing Z_0 (or decreasing R) this discontinuous transition terminates in a critical point. If the adhesion transition in the contact potential has been continuous, the finite range Z_0 now leads to a smooth crossover between the bound and the pinned state.

7. Influence of thermal fluctuations

So far, the shape of minimal energy has been considered. Vesicle membranes are rather soft and undergo thermally excited fluctuations around these minimal states. Here, we focus on the influence of these fluctuations on bound shapes and, in particular, on the adhesion transition. We discuss this for adhesion in a potential with finite range. Two different regimes must be distinguished.

(1) If the energy difference ΔF between the free and the bound state is large compared to the thermal energy T , i.e. for $|\Delta F| \gg T$, the bound state will exhibit shape fluctuations but remain bound for exponentially long time scales. A typical amplitude a for such a shape fluctuations is then given by equipartition as $\langle a^2 \rangle \sim T/\kappa$ up to some numerical factor depending on the particular mode.

(2) The more interesting case arises for $|\Delta F| \lesssim T$ where thermal activation leads to unbinding. As a definition for a characteristic depth $V^0 = V_u^0$ or a characteristic temperature T_u , we take the criterion $|\Delta F(V_u^0)| \simeq T$ or $|\Delta F(V^0)| \simeq T_u$. With (13) and (14), we find in the long-ranged and the pinned case

$$V_u^0 \sim \begin{cases} T/R^2 & \text{for } R \lesssim Z_0 \\ T/(RZ_0) & \text{for } Z_0 \ll R \lesssim R_c \equiv (\kappa/T)Z_0. \end{cases} \quad (16)$$

The length scale R_c arises from the consistency requirement that $V^0 < V_a^0 \simeq W_a$, which was assumed when using the estimate (14) for ΔF . The breakdown of this relation for $R > R_c$ indicates that large vesicles will not enter the pinned regime because the energy gain ΔF of such a pinned state would be smaller than the thermal energy T . Therefore, these large vesicles unbind at values of the potential depth V^0 for which the analysis at $T = 0$ predicts bound vesicles with a finite contact area. This regime $R > R_c$ can also be attacked from a different point of view as follows.

Consider an *open* membrane bound to a wall by a potential which decays faster than $\sim Z^{-2}$. Since the wall restricts the fluctuations, the bound membrane has lower entropy than a free membrane. This loss leads to an entropic repulsion and, thus, to a fluctuation induced unbinding at a finite potential depth $V_{u,open}^0$ [6,17]. For a two-parameter potential with range Z_0 and depth V^0 the critical amplitude $V_{u,open}^0$ scales like [18]

$$V_{u,open}^0 \sim T^2/(\kappa Z_0^2). \quad (17)$$

Bound *closed* vesicles also experience an entropic loss in the contact zone. One might therefore expect that $V_{u,open}^0$ also gives the critical amplitude for the unbinding in this case provided the vesicle is indeed bound with a finite fraction of its area to the wall for $T = 0$. This latter condition restricts the whole argument to vesicles with such a size that $V_a^0(R) < V_{u,open}^0$. This relation is fulfilled for $R > R_c$ with the same crossover radius R_c appearing already in (16).

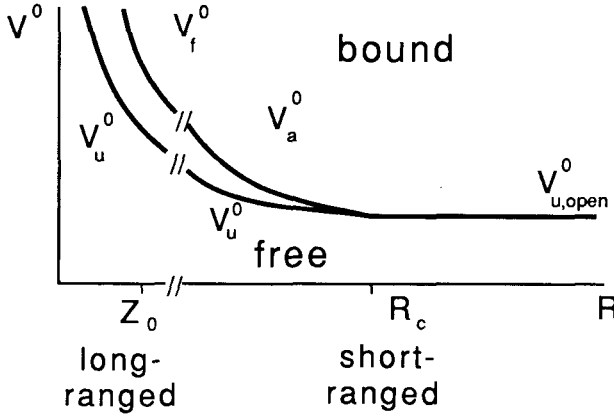


Fig.2: Schematic phase diagram for adhesion in a potential with finite range at finite temperature T . Depending on the three length scales Z_0, R and R_c , three different regimes must be distinguished for the unbinding: (1) In a long-ranged potential ($R \lesssim Z_0$), decreasing the potential depth V^0 first leads to a smooth crossover at $V^0 \simeq V_f^0$ where the bound shape changes its shape from the deformed to a nearly free shape. Finally, the vesicle unbinds via thermal activation at $V^0 \simeq V_u^0$. (2) In a short-ranged potential ($Z_0 \ll R$), small vesicles with $R < R_c$ first undergo the curvature driven transition from a bound state with finite contact area to the pinned state with the nearly free shape for $V^0 \simeq V_a^0$. These small vesicles then unbind via thermal activation at $V^0 \simeq V_u^0$. (3) Large vesicles with $R > R_c$, cannot enter the regime of pinned states since they unbind via shape fluctuations in the contact zone at $V^0 \simeq V_{u,open}^0$.

For this crossover length R_c , we find $R_c = 0.1 \mu m$ with the typical values $Z_0 = 4 nm$ and $\kappa/T = 25$. Although there is uncertainty about the numerical prefactor, this crossover seems to be below the optical resolution. It might, however, be shifted to larger values using multi-lamellar vesicles because κ is proportional to the number of bilayers.

A possible objection against the use of (17) as the characteristic strength for the unbinding of closed vesicles concerns the effect of constraints, in particular of the area constraint. Such a constraint will typically create a lateral tension which acts to suppress the shape fluctuations and, thus, to reduce the entropic loss in the contact zone. In the presence of such a tension one has $V_{u,open}^0 = 0$ provided the interaction potential $V(Z)$ decays as a power law for large Z [4].

The estimates given in this section for the adhesion transition of vesicles lead to three different regimes as shown and described in Fig.2.

8. Conclusion

All phenomena discussed here show a characteristic dependence on the size, R , of the vesicle which arises from the interplay of the bending energy $\sim \kappa$ and the adhesion

energy $\sim WR^2$.

For 'strong' adhesion, with $R \gg (\kappa/W)^{1/2}$, the contact potential is well suited (i) to describe bound shapes, (ii) to clarify the notion of an effective contact angle and (iii) to discuss topological changes of bound states. For 'weak' adhesion, with $R \simeq (\kappa/W)^{1/2}$, we find an adhesion transition. Although this phenomenon occurs already for a contact potential, one has to study a finite range potential in order to determine the critical behaviour at this transition.

How vesicles unbind, depends on their size. Small vesicles undergo a curvature driven transition from a bound to a pinned state from which they unbind by thermal activation; large vesicles unbind via shape fluctuations.

The theoretical predictions described here should be accessible to experiments. For a verification of the condition (2) for the contact curvature, reflection interference microscopy seems to be a promising technique [19]. Transitions between different bound shapes as well as the adhesion transition could be induced and analysed by changing the temperature or the osmotic conditions, compare Ref.11 and 12 where such an approach has been applied for free vesicles.

Acknowledgement

We thank D. Beysens, N. Boccara and G. Forgasz for the invitation to this exciting workshop.

REFERENCES

- [1] For a review, see, E. Evans, *Colloids and Surfaces* **43** 227 1990.
- [2] See, e.g., R. M. Servuss and W. Helfrich, *J. Phys. France* **50** 809 1990.
- [3] U. Seifert and R. Lipowsky, *Phys. Rev. A* **42** 4768 1990.
- [4] R. Lipowsky and U. Seifert, *Langmuir* in press .
- [5] R. Lipowsky and U. Seifert, *Mol. Cryst. Liq. Cryst.* in press .
- [6] For a recent review, see, R. Lipowsky, *Nature* **349** 475 1991.
- [7] P.B. Canham, *J. Theoret. Biol.* **26** 61 1970.
- [8] W. Helfrich, *Z. Naturforsch.* **28c** 693 1973.
- [9] E. Evans, *Biophys. J.* **14** 923 1974.
- [10] S. Svetina and B. Zeks, *Eur. Biophys. J.* **17** 101 1989.
- [11] U. Seifert, K. Berndl and R. Lipowsky, *Phys. Rev. A* in press .
- [12] K. Berndl, J. Käs, R. Lipowsky, E. Sackmann and U. Seifert, *Europhys. Lett.* **13** 659 1990.
- [13] E. Evans and D. Needham, *J. Phys. Chem.* **91** 4219 1987.
- [14] G. Cevc, W. Fenzl and L. Sigl, *Science* **249** 1161 1990.
- [15] E. Evans, *Biophys. J.* **48** 175 1985.
- [16] U. Seifert, *Phys. Rev. A* in press .
- [17] R. Lipowsky and S. Leibler, *Phys. Rev. Lett.* **56** 2541 1986.
- [18] R. Lipowsky and B. Zielinska, *Phys. Rev. Lett.* **62** 1572 1989.
- [19] A. Zilker, H. Engelhardt and E. Sackmann, *J. Phys. France* **48** 2139 1987.